



NIH Public Access

Author Manuscript

Anal Chem. Author manuscript; available in PMC 2010 October 1.

Published in final edited form as:
Anal Chem. 2009 October 1; 81(19): 7944–7953. doi:10.1021/ac901030k.

Monitoring Dynamic Changes in Lymph Metabolome of Fasting and Fed Rats by Electrospray Ionization-Ion Mobility Mass Spectrometry (ESI-IMMS)

Kimberly Kaplan[†], Prabha Dwivedi[†], Sean Davidson[‡], Qing Yang[‡], Patrick Tso[‡], William Siems[†], and Herbert H. Hill Jr.^{*,†}

[†]Washington State University, Pullman, Washington 99164

[‡]University of Cincinnati, Cincinnati, Ohio 45221

Abstract

Ambient pressure ion mobility time-of-flight mass spectrometry (IMMS) has recently emerged as a rapid and efficient analytical technique for applications to metabolomics. An important application of metabolomics is to monitor metabolome shifts caused by stress due to toxin exposure, nutritional changes, or disease. The research presented in this paper uses IMMS to monitor metabolic changes in rat lymph fluid caused by dietary stresses over time. Extracts of metabolites found in the lymph fluid collected from dietary stressed rats were subjected to analysis by electrospray (ESI) IMMS operated both in positive and negative ion detection mode. Metabolites detected were tentatively identified based on their mass to charge ratio (m/z). In one sample, 1180 reproducible tentative metabolite ions were detected in negative mode and 1900 reproducible tentative metabolite ions detected in positive mode. Only biologically reproducible ions, defined as metabolite ions that were measured in different rats under the same treatment, were analyzed to reduce the complexity of the data. A metabolite peak list including m/z , mobility, and intensity generated for each metabolome was used to perform principle component analysis (PCA). Dynamic changes in metabolomes were investigated using principle components PC1 and PC2 that described 62% of the variation of the system in positive mode and 81% of the variation of the system in negative mode. Analysis of variance (ANOVA) was performed for PC1 and PC2 and means were statistically evaluated. Profiles of intensities were compared for tentative metabolite ions detected at different times before and after the rats were fed to identify the metabolites that were changing the most. Mobility-mass correlation curves (MMCC) were investigated for the different classes of compounds.

Nutritional stresses and diseases such as diabetes, obesity, and eating disorders result in various metabolic changes that in turn lead to chronic illnesses such as cardiovascular disease, hypertension, and cancer. Extensive human epidemiologic data have indicated prenatal and early postnatal nutrition influence adult susceptibility to diet-related chronic diseases by affecting the adult metabolism.¹ The ability to monitor metabolome changes enables early life nutritional interventions leading to the prevention of chronic disease in humans² and provides insight into the response of a biological system subjected to genetic and environmental stresses.³ Metabolomics is a developing field with a primary focus on early disease detection and prevention by analyzing changes that occur in an organism's metabolome. A metabolome is

© XXXX American Chemical Society

*To whom correspondence should be addressed. Phone: 5093355648. hhhill@wsu.edu.

SUPPORTING INFORMATION AVAILABLE

Appendix A. Metabolites detected as positive ions. Appendix B. Metabolites detected as negative ions. This material is available free of charge via the Internet at <http://pubs.acs.org>.

defined as “the total quantitative collection of small molecular weight compounds (metabolites) present in a cell or organism which participate in metabolic reactions required for growth, maintenance, and normal function”.⁴ Metabolites represent the end product of various regulatory processes and are small molecules (<1000 Da) that range in extremes of polarity, volatility, solubility, and concentration levels.⁵ The goal for metabolomics is to do a comprehensive analysis for the whole metabolome under a certain set of conditions.⁶ Application of metabolomics to nutritional research has the potential to enhance our knowledge of human health and the interacting and regulatory roles of nutrition.⁷

Study of the lymphatic fluid of various organs has many applications including the diagnosis of cancer, the body's ability to fight infections, and intestinal fat absorption. The lymphatic system produces and transports lymph fluid from tissues to the circulatory system and thereby prevents edema. The lymphatic system is also a major part of the immune system. The mesenteric lymph from the bowel has an additional important function of transporting macromolecules and lipids, fat soluble vitamins and water insoluble compounds.⁸ Changes in mesenteric lymph composition reflect functions of maintaining fluid homeostasis and blood pressure by returning interstitial fluid back to the circulation.⁸ The lipid composition of mesenteric lymph has been studied extensively, particularly in relation to fat absorption. The lipid content of intestinal lymph fluctuates widely depending on the type, extent, and timing of fat ingestion. Target metabolites such as cholesterol,^{9,10} saturated and unsaturated fatty acids,^{11,12} glucose,^{13,14} and amino acids¹⁵ have been measured in lymph fluids using gas chromatography (GC), liquid chromatography (LC), and spectrophotometric methods.

In metabolomic analysis, the ability to measure a wide range of diverse chemicals is essential. Current analytical methods for measuring metabolomes are limited in the number of metabolites detected due to the chemical complexity of the metabolites and often multiple technologies are employed.¹⁶ Conventional instrumentation used in metabolomic studies include liquid chromatography–mass spectrometry (LC–MS),^{17,18} capillary electrophoresis–mass spectrometry (CE–MS),^{19,20} ¹H NMR²⁰ and gas chromatography–mass spectrometry (GC–MS).²¹ Electrospray ion mobility- time-of-flight mass spectrometry (ESI-IMMS) has recently been applied for metabolite profiling of *Escherichia coli* and demonstrated the detection of more than 500 metabolite features consisting of diverse chemical compounds including hydrophobic lipids, inorganic ions, volatile alcohols, and hydrophilic carbohydrates without derivatization.²²

Ion mobility spectrometry is a rapid gas phase separation technique that has commonly been used to separate small molecules such as drugs and explosives.^{23–25} IMS instruments usually have two sections, a desolvation and a drift region that are separated by an ion gate. Ions are produced at the source, enter the desolvation region, and are pulsed into the drift region. A counter flow of buffer gas is introduced into the IMS near the low voltage end of the drift tube. As ions migrate through the buffer gas under the influence of a weak electric field, they collide with the buffer gas atoms or molecules and after numerous collisions they attain a constant velocity (v_d) which is characteristic of the ion's identity. The v_d is proportional to the electric field (E) and the mobility of the ion (K) is the ratio of the ion's velocity to the electric field.

$$K = \frac{v_d}{E} = \frac{L^2}{t_d V} \quad (1)$$

This mobility, corrected for pressure (P), temperature of the drift region (T), length of the drift tube (L), and the voltage on the ion gate (V), is reported as the ion's reduced mobility constant (K_0).

$$K_0 = \frac{L^2}{Vt_d} \times \frac{273}{T} \times \frac{P}{760} \quad (2)$$

Unlike conventional methods used in metabolomics such as chromatography where analyte separation occurs based on interaction with a column or stationary phase, IMS separation is based on the collisional cross section (size) of the ions. By coupling IMS to a mass spectrometer, separation of isomers or isobars is possible.^{26,27} Separation selectivity can be achieved using different drift gases in the IMS.²⁸ There is a correlation between mobility and mass for compounds in homologous classes; for example, protonated triglycerides have a linear relationship that is different from phospholipids.²⁹ As a result, ion mobility coupled with mass spectrometry (IMMS) can separate a vast range of chemical classes into characteristic mobility-mass correlation curves (MMCC).^{30–32} Classes of compounds which have been separated with IMMS include isobaric carbohydrates as sodiated adducts, oligosaccharides,³³ isomeric peptide mixtures,³⁴ and volatile organic metabolites in human breath.³⁵

The purpose of this work is to evaluate IMMS as an analytical technique applicable to metabolomics for determining the changes in the mesenteric lymph metabolites of animals that were fasting or fed with a mixed meal using a multivariate technique for data analysis.

EXPERIMENTAL SECTION

Animal Preparation

Male Sprague-Dawley rats were used. After an overnight fast, the main mesenteric lymph duct was cannulated with vinyl tubing (0.8 mm OD) while rats were under halothane anesthesia, according to the procedure originally described by Bollman et al.³⁶ and modified by Tso et al.³⁷ In addition, a silicone tube (2.2 mm OD) was placed 2.0 cm into the duodenum through the proximal stomach. The incision in the fundus of the stomach wall was closed by a purse-string suture. The rats were placed into restraining cages, and the surrounding temperature was kept at 30 °C during the overnight recovery and the experiments the next day. Postoperatively, the animals were given a glucose-saline solution (145 mM NaCl, 4.0 mM KCl, and 0.28 M glucose) via the intraduodenal cannula at a rate of 3.0 mL/hour for 16 hours before the experiment then infusate was changed to saline. The experiments were always performed on the day after surgery.

Lymph Nutrient Treatment

On the day of the experiment, lymph was collected for one hour as the fasting sample. The saline infusion into the duodenal cannula was then replaced by 3.0 mL of Ensure, a commercially available dietary supplement from Ross Laboratories, Columbus, OH. Thirty minutes after the bolus dose of Ensure, 3.0 mL/hour of saline was infused again until the end of the experiment. Lymph fluids were collected at hourly intervals for 6 h in graduated glass tubes surrounded by ice. A total of three rats were treated, with seven samples collected per rat. The samples were placed on dry ice and shipped to Washington State University for metabolomic analysis.

Metabolite Extraction

Metabolite extraction was similar to Chen et al.³⁸ Metabolites from rat lymph were extracted in HPLC reagent grade methylene chloride purchased from J.T. Baker (Phillipsburg, NJ) using a 2:1 v/v ratio (solvent: lymph). The methylene chloride extract was evaporated to dryness with nitrogen and reconstituted with 500 µL ACS grade methanol purchased from EMD Chemicals Inc. (Gibbstown, NJ). The samples were centrifuged for 30 min at 13 kRPM. After

centrifugation, water and acetic acid were added to the supernatant (49.5:49.5:1 water:methanol:acetic acid) and was directly electrosprayed into the IMMS.

Instrumentation: ESI-IMMS

IMMS experiments were performed using an in-house constructed IMS coupled to an Ionwerks (Houston, Texas) TOF MS that is shown in Figure 1 and described elsewhere.^{39,40} Lymph extracts were directly infused through a standard polyimide coating (TSP) capillary with an I.D. of 50 μm and an O.D. of 150 μm purchased from Polymicro (Phoenix, AZ) at a flow rate of 3 $\mu\text{L}/\text{min}$ into the desolvation region of the highresolution, ambient pressure IMMS. A voltage bias from the capillary to the first ring of the IMS was kept at 3.45 kV for positive mode and -3.45 kV for negative mode conditions. IMMS experiments were conducted in both positive and negative mode. A summary of operating voltages can be found in Table 1.

Ion Mobility Spectrometer—The high resolution, ambient pressure IMS consisted of a conventional stacked-ring design. The IMS was divided into two sections using a Bradbury-Nielsen ion gate. The desolvation region was 7.5 cm and the drift region measured at 17.6 cm. The conducting rings were connected through a series of high temperature, high voltage resistors (0.5 M Ω resistors for the desolvation region and 1.0 M Ω resistors for the drift region) (CADDLOCK electronics, Inc. Riverside, CA). The electric field was 436 V/cm throughout the drift region. The ions were introduced into the drift region at a pulse width of 0.2 ms. The temperature of the IMS was set to 200 °C and the buffer gas (nitrogen) flow rate was 1 L/min throughout the tube. The calculated K_0 values were standardized to 2,4-lutidine (1.95 $\text{cm}^2\text{V}^{-1}\text{s}^{-1}$) and TNT (1.54 $\text{cm}^2\text{V}^{-1}\text{s}^{-1}$).

Time-of-flight Mass Spectrometer—A time-of-flight (TOF) mass spectrometer (coupled to the IMS) was constructed at Ionwerks Inc., Houston, TX. A low pressure interface (2.1 Torr) connected the high pressure IMS (690–703 Torr for Pullman, WA) to the TOF high vacuum ($\sim 10^{-6}$ Torr). The interface consisted of three lenses: nozzle, focus and skimmer. Ions were guided from the interface by a series of lenses and orthogonally pulsed into the 1 m reflectron flight tube and detected by a multichannel plate. Two-dimensional (2-D) spectra were acquired obtaining m/z , drift time and intensity for each ion. The TOF mass range was calibrated using 2,4-lutidine (MW 107.15) measured as a [M+H] $^+$ and maltopentaose (MW 828.73) detected as [M+Na] $^+$ for the positive mode and chloride (MW 35.45) identified as [M] $^-$ and pentatriacontanoic acid (MW 522.54) determined as [M-H] $^-$ for the negative mode.

Data Processing—Tentative metabolite assignments were accomplished based on matching m/z values with an average mass defect of ± 0.1 Da for positive mode and ± 0.07 Da for negative mode searching the human metabolome database for reported metabolites known to be in lymph fluid.⁴¹ Metabolites were also identified based on matching literature references which included glucose,^{13,14} palmitic acid (16:0),^{14,42} linoleic acid (18:2),⁴² oleic acid (18:1),⁴² and succinate.⁴³

In order to statistically analyze the 2-D IMMS data using PCA, a peak list was generated using a program created by Ionwerks that runs on IDL Virtual Machine Version 6.3 (ITT Visual Information Solutions, Boulder, CO) to obtain m/z , drift time and intensity for each ion. The drift time was used to calculate the reduced mobility, K_0 , using eq 2. Background ion peaks resulting from the electrospray solvent were masked out of the lymph metabolite spectra. Three runs were completed for one sample and reproducibility was determined for each sample. PCA analysis was performed using the demo version of PLS_Toolbox 4.2 created by eigenvector Research Incorporated (Wenatchee, WA) on Matlab Student 7.0.1.

RESULTS AND DISCUSSION

Reproducibility

Triplicate measurements, both in positive and negative ion detection mode, for metabolites present in lymph samples of a fasting rat were used to determine the reproducibility of IMMS method. After background subtraction, for negative mode 1180 reproducible tentative metabolite ions were measured with ion counts >5 , and for positive mode 1900 reproducible tentative metabolite ions were detected with ion counts >5 . Tentative metabolite ion identification is assigned since a metabolite can form more than one ion during the ionization process such as a protonated/deprotonated pseudomolecular ion, adducts or fragmentation ions. The average relative standard deviation for instrumental measurements was $\pm 0.1\%$ Da for m/z , $\pm 1\% \text{ cm}^2 \text{V}^{-1} \text{s}^{-1}$ for the K_0 and $\pm 19\%$ ion counts for the intensity. In the metabolite fingerprint of the fasting rat there were 408 ± 35 isobaric compounds separated in the negative mode along with 878 ± 102 isobaric metabolites detected in positive mode both with ion counts >5 .

Twelve fasting lymph samples from 12 different rats were analyzed in positive ion detection mode to determine the reproducibility of the variation of a biological sample. The samples were kept frozen (-40°C) until extracted. Triplicate measurements were acquired for each sample either on different days or on the same day. Between the 12 lymph extracts analyzed, 276 common metabolite peaks with ion counts >5 including 70 isobars were detected reproducibly. The average standard deviation for the intensity from the same metabolite peaks detected in all the samples was ± 16 ion counts. By only looking at the common metabolites detected in different rats, the complexity of the spectra is reduced and the metabolites seen are stable from rat to rat under the same treatment.

Metabolite Profile of Fasting and Fed Rat Lymph Samples

ESI-IMMS analysis of ESI solvent for positive mode produced ions that were identified as $[M(H_2O)_n + H]^+$, $[M + Na]^+$, $[M + K]^+$, $[M_2 + H]^+$, $[M(CH_3COOH)_n + H]^+$, and $[M + NH_4]^+$ where M was either water, methanol, or acetic acid and for negative mode produced ions that were identified as $[M(H_2O)_n + OH]^-$, $[M + HCOO]^-$, $[M + CH_3COO]^-$, $[M + NO_2]^-$, $[M + NO_3]^-$ or $[M + Cl]^-$ where M was either water or methanol. Seven aliquots of lymph samples constituting one fasting stage and six at one hour intervals after feeding were collected from three different rats and analyzed by IMMS. Shown in Figure 2 are IMMS plots for electrospray solvent (A), fasting (B), an hour after feeding (C), and two hours after feeding (D) metabolome fingerprints for both positive and negative mode. The positive mode is shown by the pink overlay with the pink dotted line trace, and the negative mode is shown by the blue contours with the black trace. The m/z is on the x-axis and the mobility spectra on the y-axis. In each IMMS spectra there are two dotted black lines through the contours representing the average drift time for negative (1) and positive (2) ion detection. Overall, negative ions have a longer drift time indicating they are larger than positive ions. Negative ions (anions) have an extra electron and are larger due to electron-electron repulsion forces that cause them to spread further apart, and the electrons out number the protons; therefore, the protons cannot pull the extra electrons as tightly toward the nucleus. Positive ions (cations) are smaller due to the less electron-electron repulsion and the ability to pull fewer electrons toward the nucleus more tightly.

Bioinformatics for Metabolite Fingerprints

Analytical data from metabolome profiles are complex and multivariate. They consist of observations of many different metabolites for a number of compounds.⁴⁴ Data interpretation is accomplished by multivariate treatments that are conducted by either supervised or unsupervised methods. A common unsupervised method is principle component analysis (PCA) used to identify patterns in the data. The rationale for using PCA was to determine if

there were pattern differences among samples. PCA has recently been used to demonstrate the effect of different diets metabolites from rat urine.⁴⁵ Principal component analysis (PCA) was performed on seven lymph metabolome fingerprints (Fasting, Time 1, Time 2, Time 3, Time 4, Time 5, and Time 6) for three different rats detected by IMMS for both positive and negative ion mode detection. PCA was performed on the metabolites that did not vary biologically in all three rats. IMMS data was initially converted into a multidimensional table with the variables being identified metabolites at the concentration detected in a sample. For positive ion detection mode there were 165 metabolite ions (variables) shown in Supporting Information (SI) Appendix A and in the negative mode there were 78 metabolite ions (variables) shown in SI Appendix B. The first principal component (PC) was created by drawing a new coordinate axis that represents the new direction of maximum variation through the multidimensional data (line of best fit). The second PC must be orthogonal to the first PC and describe the maximum remaining variability and subsequent PCs must be orthogonal to the previous PC. The data was then projected onto PC1 and PC2 to create a score plot that represents the best 2-D window into the original 165-dimensional data for the positive mode or 78-dimensional data for the negative mode.

The PCA score plots for positive and negative mode are shown in Figure 3. Each sample has three data points that represent three different rats indicated by the same marker. Tight clustering of the points among the three different rats is evident by looking at the biological reproducibility of the concentration of the metabolites. Both ionization mode score plots show a circular pattern between PC1 and PC2 as the rats are fed; this pattern indicates the metabolome shifts once fed and after six hours cycles back to fasting. For positive mode, the first two PCs accounted for 62% of the variation in the system. Fasting, Time 1, Time 6, and Time 5 cluster close together, whereas Time 2 does not show similarities to any other times and Time 3 and Time 4 are in the same quadrant. After the rats are fed, their metabolome shifts the furthest after two hours and cycles back to fasting after six hours. A statistical software (Proc Mixed) was run to assess whether the assumption of compound symmetry was satisfied and to assess whether there were any differences between the means for each time period. The assumptions were satisfied for both analyses and the ANOVA indicated that there was a significant difference between the means for each principal component (PC1: P value <0.0001; PC2: P value <0.0001). In addition, multiple comparisons (Fisher's LSD) indicated that all individual means differed for PC1 and PC2 (P < 0.05), except the means for Times 1 and 5; Fasting and Time 6 did not differ for PC1 and Times 5 and 6 for PC2.

In negative mode, the first two PCs accounted for about 81% of the variation in the system. These two PCs also showed a circular pattern among the observations. In negative mode, Time 1 shows the greatest perturbation from Fasting. Following a counterclockwise pattern, Times 2 and 3 come next and cluster together, Times 4 and 5 groups; and Fasting and Time 6 overlap. Proc Mixed was also run and the assumption of compound symmetry was satisfied for both analyses and the ANOVA indicated that there was a significant difference between the means for each principal component (PC1: P value <0.0001; PC2: P value <0.0001). In addition, multiple comparisons (Fisher's LSD) indicated that all individual means differed from each other (P < 0.05), except that the means for times Fasting and 6; 2 and 3; 4 and 5; Fasting and 5; and 5 and 6 did not differ for PC1; and times Fasting and 6; 2 and 3; 4 and 5; Fasting and 1; and 1 and 6 did not differ for PC2.

The tight grouping of the different rats and the clear cycle pattern for the different times before and after feeding indicates that dietary stresses can rapidly be determined by the analysis of their metabolome. With IMMS individual metabolites were identified and the metabolites responsible for the change in PCA can be determined.

IMMS Metabolite Profiling

One of the advantages of IMMS is that changes in many individual metabolites can also be simultaneously monitored. For example, Figure 4 plots the intensity of positive ions produced from sets of metabolites found in the spectra for each time interval. In this figure they are organized based on class where the alcohols and polyols are shown in Figure 4a; amino acids in Figure 4b; carbohydrates in Figure 4c; glycerolipids in Figure 4d; monoacylglycerol in Figure 4e; and fatty acids in Figure 4f. Similarly, Figure 5 plots the intensity of negative ions produced from sets of metabolites found in the spectra for each time interval. In this Figure, Figure 5a is of carbohydrates; Figure 5b is of carnitines; Figure 5c is of unsaturated fatty acids; and Figure 5d is of saturated fatty acids.

From these figures it is clear that concentrations of different metabolites are changing with time. For example, as shown in Figure 4a, glycerol reaches a maximum at 3 h. Increase in the glycerol concentration in the lymph is consistent with fatty acid metabolism where triacylglycerols are broken down into fatty acids and glycerol. In addition changes in diglyceride (DG) (22:2/14: 0) have a maximum after 3 h along with pentacosanoic acid and linoleic acid shown in Figure 4d, 4f, 5c, respectively. Another example in which the metabolic dynamics can be followed is illustrated in Figure 4c. Here glucose is seen to decrease as amylose increases. This is consistent with studies by Goddard, Young, and Marcus (1984), in which they found that increased concentration of amylose from rice decreased concentrations of glucose in humans.⁴⁶ The amino acids detected are shown in Figure 4b where the amino acid derivative 2-aminoisobutyric acid is the most predominant amino acid detected. Three essential amino acids were measured: phenylalanine, tryptophan, and valine. Essential amino acids are only obtained by ingestion.

Mobility-Mass Correlation Curve

Another major advantage to IMMS is the correlation between mass and mobility,⁴⁷ also known as mobility-mass correlation curves (MMCC), for compounds in homologous classes. Once the metabolites were tentatively identified based on mass, MMCC plots were created for the different classes identified shown in Figure 6. On the x-axis is the m/z and on the y-axis $1/K_0$. All MMCCs were created using data found in SI Appendix A and B. For positive mode there were 20 different classes determined from the metabolites detected ($N > 3$) in the dietary stressed lymph samples. The lines for best fit to the data are shown in Figure 6A and C and the equation, R^2 and numbers of metabolites used to create the lines (N) is shown in Table 2. IMMS spectra of five amino acids and glucose as different ions are shown in Figure 6B of a metabolite profile from a fasting rat. IMMS spectra of diglycerides and triglycerides are shown in Figure 6D that make up the glycerolipid MMCC. For negative mode there were six different classes determined from metabolites identified ($N > 3$) from the 21 lymph samples. The MMCCs are shown in Figure 6E and the equation for the line; R^2 and N are shown in Table 2. IMMS spectra of unsaturated and saturated fatty acids and different sugar ions are shown in Figure 6F. The MMCC can be used as a predictive tool to determine the class of an unknown compound that can lead to the unknown identity.

IMMS Application to Quantification

Quantification of metabolites by direct infusion ESI is difficult due to matrix interfaces. Isotope dilution methods are difficult with very complex biological samples in mass spectrometry due to chemical interferences at virtually every mass. Thus the traditional method for quantification with electrospray MS requires coupling slow, chromatographic separations to mass spectrometers. Because high resolution IMS separates ions into mobility space and reduces interferences from chemical noise, isotopes of compounds can be clearly seen on the mobility separated mass axis. IMMS spectra for negative mode is shown in Figure 7 with a zoom region of glucose with chlorine adduct. The isotope ratio of ^{35}Cl and ^{37}Cl is clearly demonstrated in

the zoom section. By adding known amounts of nonradioactive isotopes and separating them in mobility space, accurate response factors can be determined from the isotope and used to correct for matrix effects. Thus the use of isotope dilution methods using nonradioactive isotopes should enable quantitative analyses by IMMS when used with direct infusion ESI or with ambient pressure MALDI with IMMS.^{48,49}

CONCLUSION

IMMS is a rapid, comprehensive analytical technique that can be applied in conjunction with statistical analysis to the study of dynamic changes in metabolomes due to external stresses. The IMMS used in this study was a reproducible technique where the average deviation determined for the metabolites detected from the triplicate measurements was $\pm 0.1\%$ Da for m/z , $\pm 1\% \text{ cm}^2\text{V}^{-1}\text{s}^{-1}$ for K_0 , and $\pm 19\%$ for intensity. IMMS can reproducibly detect 1180 metabolite ions in negative mode and 1900 metabolite ions in positive mode with ion counts >5 in one sample. With a simple extraction technique and analyzing metabolites that are found in the same treatment using three different rats, 165 metabolites were detected in positive mode analyses of the lymph samples and 78 metabolites in the negative mode analyses of the lymph samples. Principal component analysis was used on IMMS data, and a circular pattern was observed for both ion detection modes. The lymph metabolomes show a distinct perturbation after being fed and then cycle back to the initial fasting time for both positive and negative ion detection mode.

In the negative mode the predominant metabolites detected included saturated and unsaturated fatty acids and sugars, whereas in the positive, mode the most abundant metabolites were amino acids, sugars, triglycerides, and diglycerides. Classification of metabolites was achieved using IMMS based on MMCCs. By developing a database using classes of standards (such as a series of varying carbon numbers in fatty acids), MMCCs would improve ion identification instead of using m/z values alone.

Ion mobility mass spectrometry has the ability to reproducibly provide rapid separation to complex biological samples and is a new rising analytical technique for the assessment of metabolomes. Further investigation into different metabolomics applications would significantly enhance the potential of ESI-IMMS.

Acknowledgments

This project was supported in part by a research grant from Department of Health and Human Service: Public Health Services organization (Road Map Grant No. R21 DK070274). We acknowledge the work performed by the Cincinnati Mouse Metabolic Phenotype Center support by DK 59630. We also thank Dr. Marc Evans, Professor of Statistics at Washington State University, for help with the PCA interpretation.

References

1. Leon D. Eur. J. Clin. Nutr 1998;52:S78–S82.
2. Waterland RA, Jirtle RL. Nutrition 2004;20:63–68. [PubMed: 14698016]
3. Fiehn O. Plant Mol Biol 2002;48:155–171. [PubMed: 11860207]
4. Dunn WB, Bailey NJ, Johnson HE. Analyst 2005;130:606–625. [PubMed: 15852128]
5. Hollywood K, Brison D, Goodacre R. Proteomics 2006;6:4716–4723. [PubMed: 16888765]
6. Goodacre R, Vaidyanathan S, Dunn WB, Harrigan GG, Kell DB. TRENDS Biotechnol 2004;22:245–252. [PubMed: 15109811]
7. Gibney MJ, Walsh M, Brennan L, Roche HM, German B, van Ommen B. Am. J. Clin. Nutr 2005;82:497–503. [PubMed: 16155259]
8. Fanous M, Phillips A, Windsor J. JOP. J Pancreas 2007;8(4):374–399.
9. Chu, S-h; Hegsted, DM. J. Nutr 1980;110:2198–2206. [PubMed: 7431120]

10. Vine D, Croft K, Beilin L, Mamo J. *Lipids* 1997;32:887–893. [PubMed: 9270982]
11. EE LC, Zheng S, Yao L, Tso P. *Am. J. Physiol. Gastrointest Liver Physiol* 2000;279:G325–G331. [PubMed: 10915641]
12. Jeffery N, Sanderson P, Newsholme E, Calder P. *Nutr. Res. (N.Y.)* 1998;18:299–308.
13. Wu G, Field CJ, Marliss EB. *Am J Physiol Endocrinol Metab* 1991;260:E141–E147.
14. Otton R, Mendonca J, Curi R. *J. Endocrinol* 2002;174:55–61. [PubMed: 12098663]
15. Ardawi MS, Newsholme EA. *Biochem. J* 1983;212(3):835–842. [PubMed: 6882397]
16. Goodacre R. *J. Nutr* 2007;137:259S–266S. [PubMed: 17182837]
17. Bedair M, Sumner L. *Trends Anal Chem* 2008;27:238–250.
18. Plumb R, Stumpf C, Granger J, Castro-Perez J, Haselden J, Dear G. *Rapid Commun. Mass Spectrom* 2003;17(23):2632–2638. [PubMed: 14648901]
19. Soga T, Ohashi Y, Ueno Y, Naraoka H, Tomita M, Nishioka T. *J. Proteome Res* 2003;2:488–494. [PubMed: 14582645]
20. Dunn W, Ellis D. *Trends Anal. Chem* 2005;24:285–294.
21. Sheperd T, Dobson G, Verrall S, Conner S, Griffiths DW, McNicol JW, et al. *Metabolomics* 2007;3:475–488.
22. Dwivedi P, Wu P, Klopsch S, Puzon G, Xun L Jr. *Metabolomics* 2008;4:63–80.
23. Eiceman, G.; Karpas, Z. *Ion Mobility Spectrometry*. 2nd ed.. Boca Ranton, FL: Taylor & Francis Group; 2005.
24. Ewing R, Atkinson D, Eiceman G, Ewing G. *Talanta* 2001;54:515–529. [PubMed: 18968275]
25. Louis R, Hill HH, Eiceman GA. *Crit. Rev. Anal. Chem* 1990;21:321–355.
26. Dwivedi P, Bendiak B, Clowers B, Hill HH. *J. Am. Soc. Mass Spectrom* 2007;18(7):1163–1175. [PubMed: 17532226]
27. Clowers B, Dwivedi P, Steiner W Jr. *Am. Soc. Mass Spectrom* 2005;16:660–669.
28. Asbury R, Hill HH. *Anal. Chem* 2000;72(3):580–584. [PubMed: 10695145]
29. Jackson S, Wang H-Y, Woods AS, Ugarov M, Egan T, Shultz AJAM. *Soc. Mass Spectrom* 2005;16:133–138.
30. Steiner W, Clowers B, English W, Hill HH. *Rapid Common. Mass Spectrom* 2004;18(8):882–888.
31. Jackson S, Ugarov M, Post J, Egan T, Langlais D, Schultz A, Woods A. *J. Am. Soc. Mass Spectrom* 2008;19:1655–1662. [PubMed: 18703352]
32. Beegle L, Kanik I, Matz L, Hill HH. *Anal. Chem* 2001;73(13):3028–3034. [PubMed: 11467550]
33. Liu Y, Clemmer DE. *Anal. Chem* 1997;69:2504–2509.
34. Wu C, Siems WF, Klasmeier J Jr. *Anal. Chem* 2000;72:391–395. [PubMed: 10658335]
35. Ruzsanyi V, Baumbach JI, Sielemann S, Litterst P, Westhoff M, Freitag L. *J. Chromatogr. A* 2005;1084:145–151. [PubMed: 16114247]
36. Bollman J, Cain J, Grindlay J. *J. Lab. Clin. Med* 1948;33(10):1349–1352. [PubMed: 18886337]
37. Tso P, Balint J, Bishop M, Rogers J. *Am. J. Physiol* 1981;241:G487–G497. [PubMed: 7325240]
38. Chen I, Shen C-S, Sheppard A. *JOACS* 1981;58:599–601.
39. Steiner WE, Clowers BH, Fuhrer K, Gonin M, Matz L, Siems WF, Schultz A, Hill HH Jr. *Rapid Commun. Mass Spectrom* 2001;15:2221–2226. [PubMed: 11746889]
40. Steiner W, English W Jr. *Anal. Chim. Acta* 2005;532:37–45.
41. Wishart DS, Tzur D, Knox C, Eisner R, ChiGuo A, Young N, et al. *Nucleic Acids Res* 2007;35:D521–D526. [PubMed: 17202168]
42. Renner F, Samuelson A, Rogers M, Glickman R. *J. Lipid Res* 1986;27:72–81. [PubMed: 3083032]
43. Helmreich E, Kipnis D. *J. Biol. Chem* 1962;237:2582–2589. [PubMed: 13906342]
44. Jolliffe, IT. *Principal Component Analysis*. New York: Springer-Verlag; 2002.
45. Gu H, Chen H, Pan Z, Jackson A, Talaty N, Xi B, et al. *Anal. Chem* 2007;79(1):89–97. [PubMed: 17194125]
46. Goddard MS, Young GB, Marcus RM. *Am. J. Clin. Nutr* 1984;39:388–392. [PubMed: 6364775]
47. Karasek F, Denney D, DeDecker E. *Anal. Chem* 1974;46(8):970–973.

48. Shumate C, Hill HH. *Anal. Chem* 1989;61(6):601–606. [PubMed: 2729593]
49. Steiner W, Clowers B, English W, Hill HH. *Rapid Commun. Mass Spectrom* 2004;18:882–888.

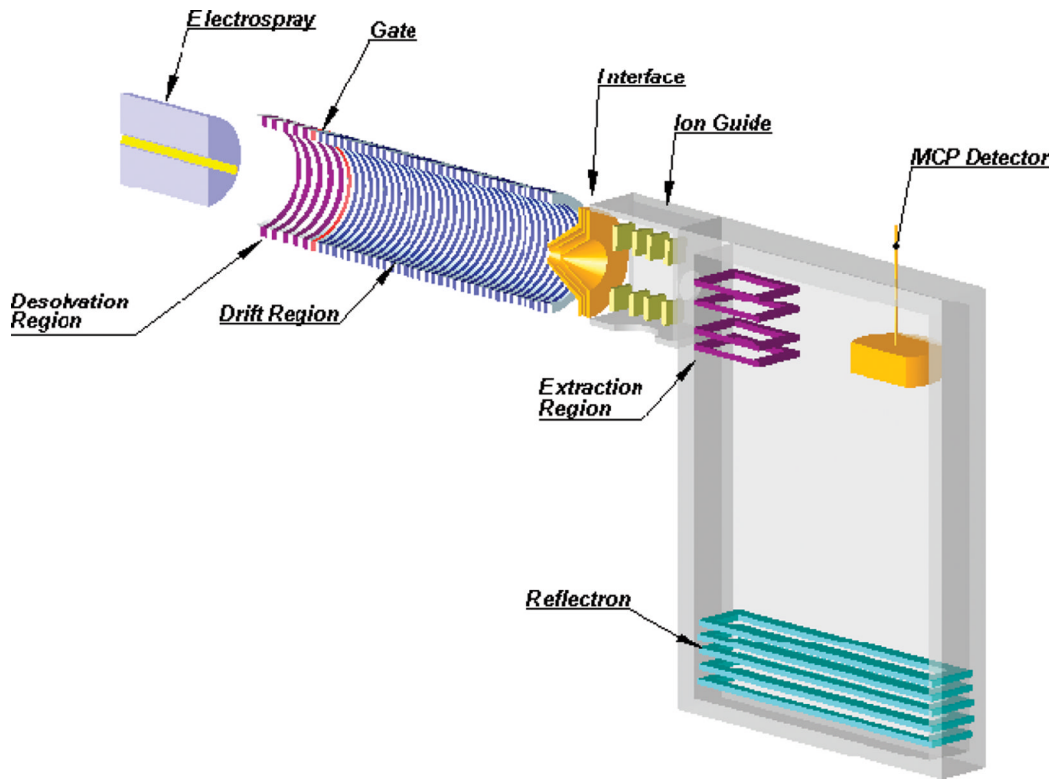


Figure 1.

Schematic of ion mobility/time-of-flight mass spectrometer (IMMS). Ions are formed in the electrospray process into the desolvation region of the ion mobility tube, gated into the drift region where they are separated based on size/charge and pulsed orthogonally into the time-of-flight mass spectrometer where they are separated on mass/charge. Two-dimensional IMMS data were acquired and for every ion mobility measurement there were 1000 mass measurements.

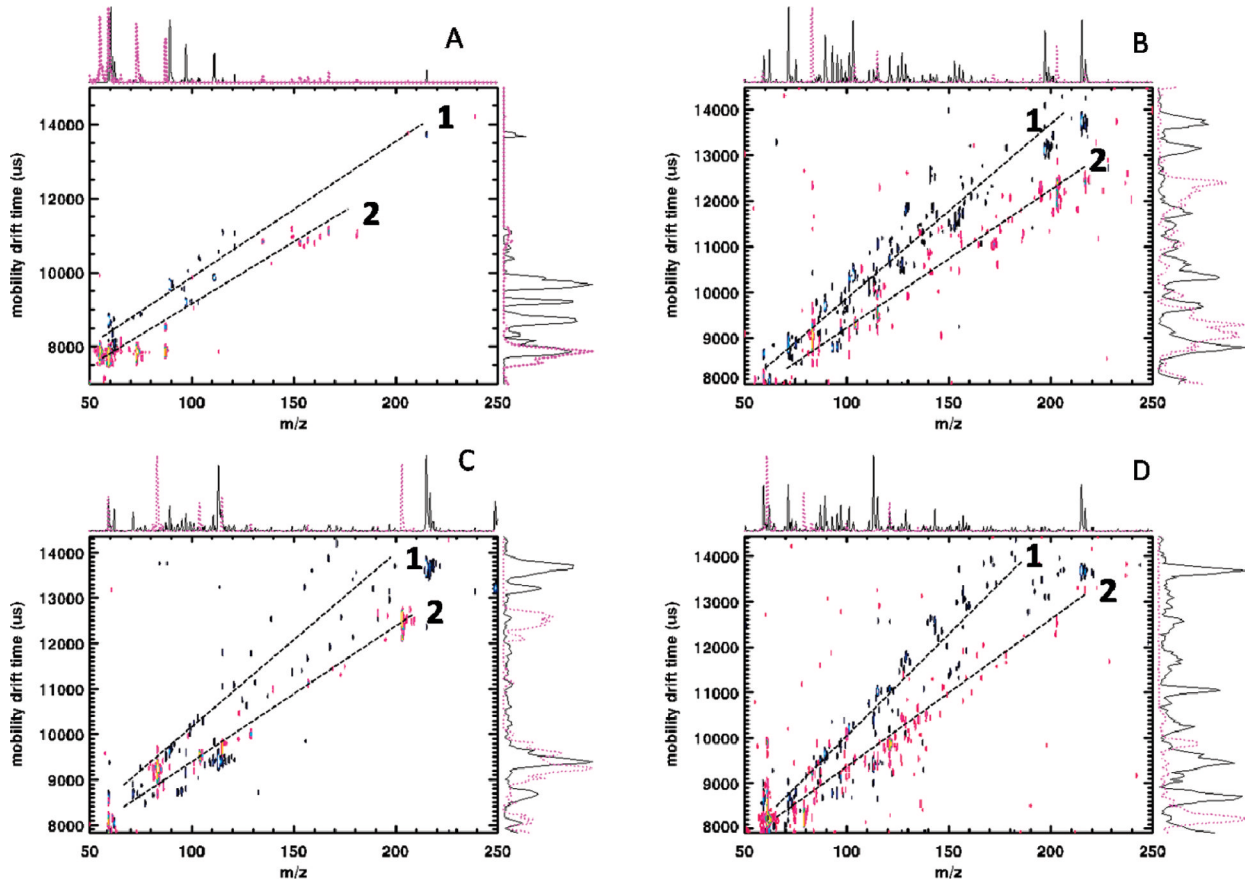
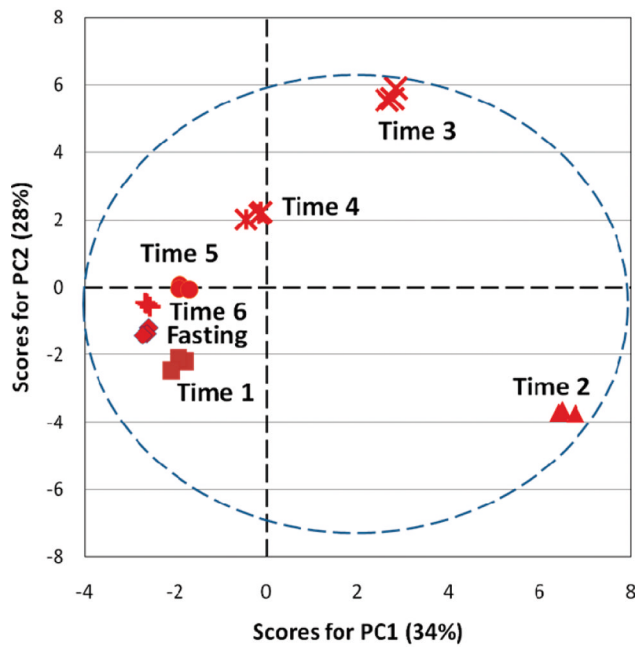


Figure 2.
IMMS contour plots for solvent background (A), fasting (B), an hour after feeding (C), and two hours after feeding (D) metabolites. Positive ion detection is shown as the pink (1) overlay with the pink contours representing tentative metabolite ions and negative ion detection is the blue contours with the black trace (2). The overall mobility-mass trend of the negative metabolite ions detected (1) has a longer drift time than the positive mode ions (2) demonstrated by the two dashed lines drawn through the average drift times for both modes.

Positive Mode



Negative Mode

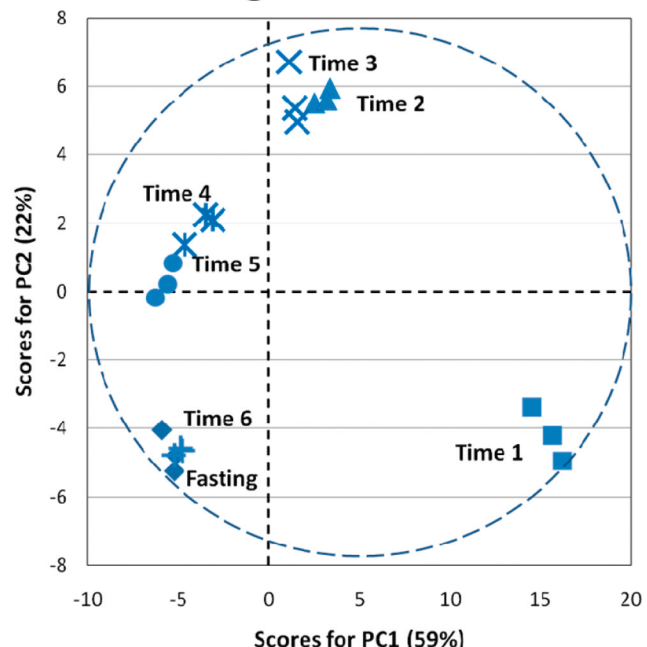


Figure 3.

Principal component analysis score plots from IMMS data collected in positive and negative mode.

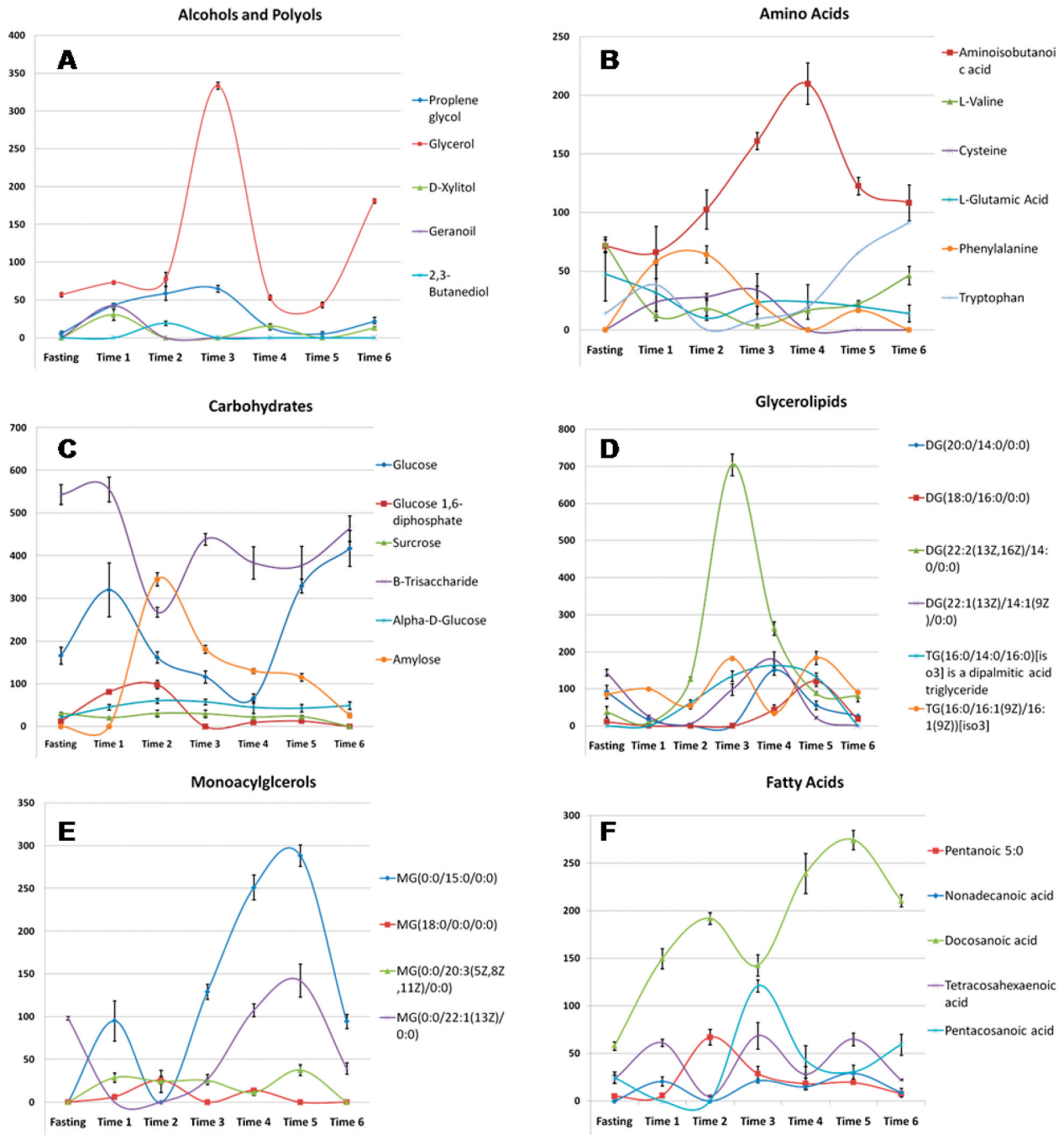


Figure 4.
Intensity profiles for specific metabolites grouped by class detected in positive mode for fasting, 1, 2, 3, 4, 5, and 6 hours after feeding.

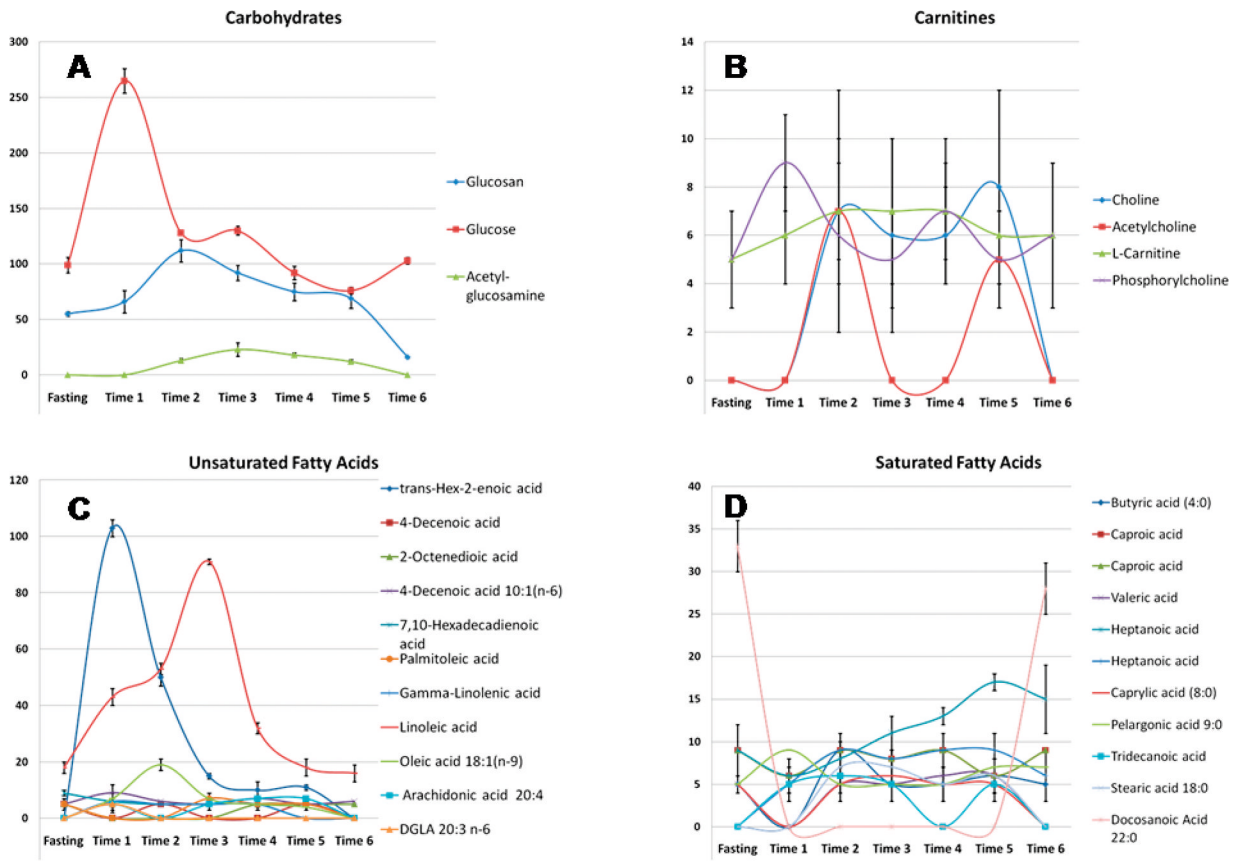
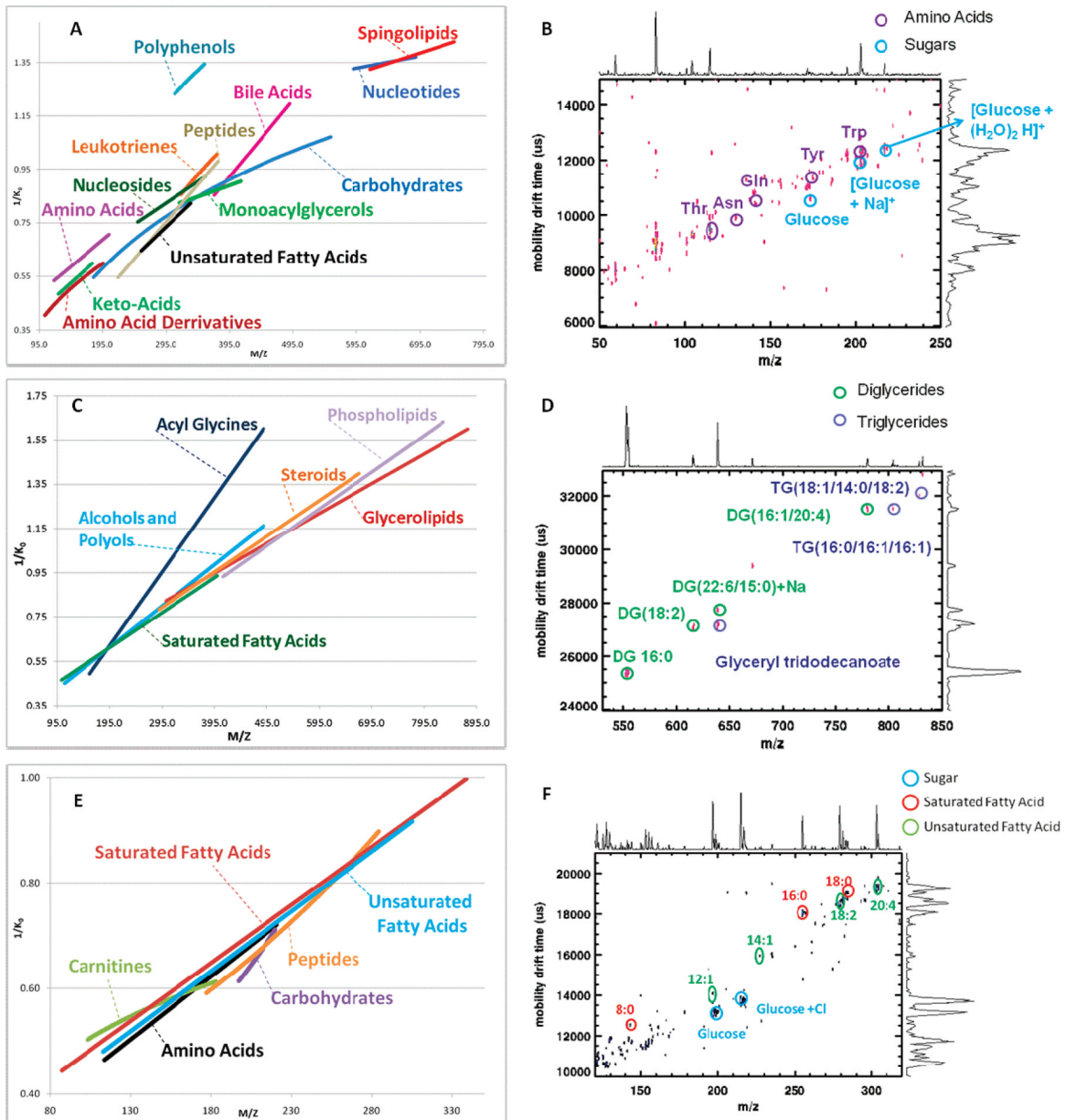


Figure 5.
Intensity profiles for specific metabolites grouped by class detected in negative mode for fasting, 1, 2, 3, 4, 5, and 6 hours after feeding.

**Figure 6.**

MMCCs of lymph metabolites detected by IMMS for positive (A, B, C, and D) and negative (E and F) mode. IMMS spectrum in positive mode for five amino acids and three glucose ions detected (B). IMMS spectrum (D) is for glycerolipids. IMMS spectrum of negative ion detection mode for three saturated fatty acids, and four unsaturated fatty acids (F).

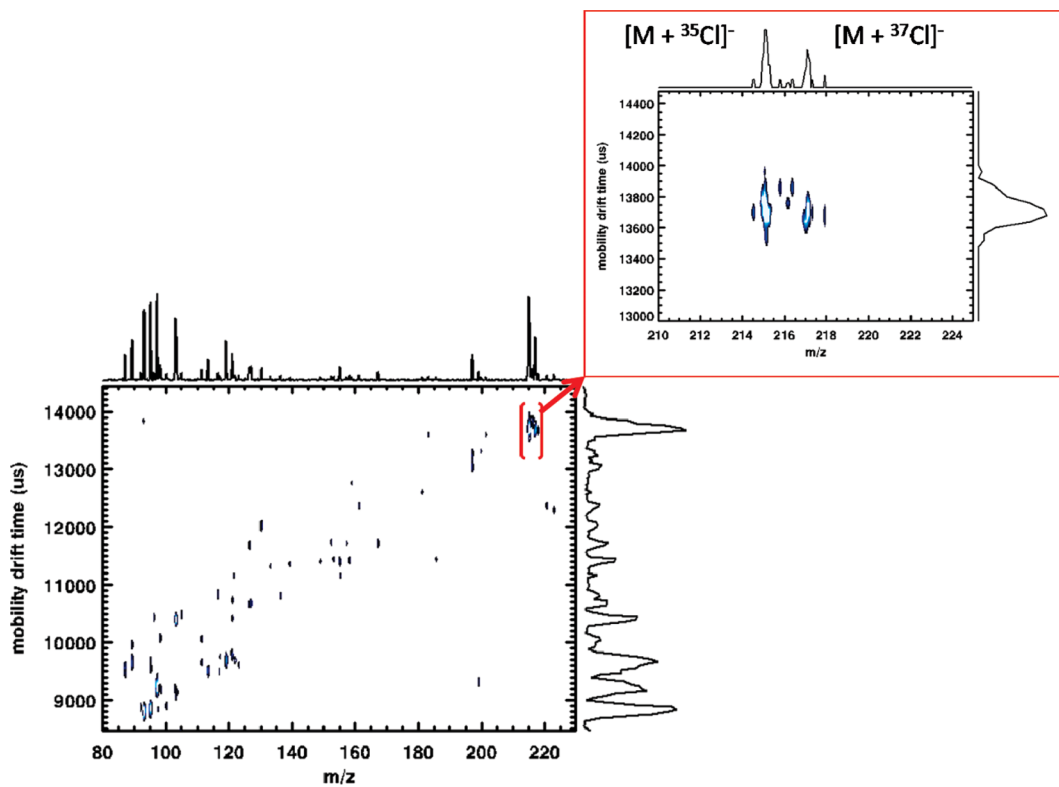


Figure 7.

IMMS metabolome profile in negative detection mode. Zoom demonstrates isotope patterns for chloride adduct with glucose. This shows potential for quantification using isotope dilution with IMMS.

Table 1

Summary of Voltages for IMMS in both Positive and Negative Mode

	positive mode voltages (V)	negative mode voltages (V)
ESI needle voltage bias	3450.00	-3450.00
gate voltage	8090.00	-8090.00
voltage on the last ring	280.60	-280.60
nozzle	87.35	-99.19
focus	104.42	-70.87
skimmer	116.20	-112.90
lens 1	12.30	-11.65
lens 2	32.20	-43.90
lens 3	-80.40	-60.40
deflector up	-0.50	0.05
deflector down	0.50	-0.50
reflector grid	969.50	-969.40
reflector back	-361.50	386.10
MCP front	4500.00	-4500.00
MCP bias	2320.00	-2320.00

Table 2IMMS Correlation Curve Equations, R^2 and Number of Peaks Mass Identified for Positive and Negative Mode

class	equation	R^2	N
positive mode			
acyl glycines	$y = 0.0033x - 0.0327$	0.9991	4
alcohols and polyols	$y = 0.0019x + 0.249$	0.9998	6
amino acids	$y = 0.002x + 0.3012$	0.9434	7
amino acid derivatives	$y = 0.3082\ln(x) - 1.0273$	0.8716	6
bile acids	$y = 0.0029x - 0.2107$	0.8272	6
carbohydrate	$y = 0.4706\ln(x) - 1.9016$	0.9183	18
carnitines	$y = 0.0014x + 0.3192$	0.9967	5
glycerolipids	$y = 0.0013x + 0.4154$	0.8742	15
keto-acids	$y = 0.0022x + 0.214$	0.9719	3
leukotrienes	$y = 0.4706\ln(x) - 1.9016$	0.7259	5
monoacylglycerol	$y = 0.1055x^{0.357}$	0.6404	5
nucleosides	$y = 0.0016x + 0.3556$	0.9279	3
nucleotides	$y = 0.0004x + 1.0627$	0.9997	3
peptides	$y = 0.0028x - 0.0629$	0.9649	4
phospholipid	$y = 0.0017x + 0.2497$	0.9717	8
polyphenols	$y = 0.0348x^{0.622}$	0.4786	5
saturated fatty acid	$y = 0.0016x + 0.303$	0.9043	9
sphingolipid	$y = 0.0008x + 0.8467$	0.977	4
steroids	$y = 0.0016x + 0.3203$	0.9674	9
unsaturated fatty acid	$y = 0.0023x + 0.0657$	0.9845	6
negative mode			
amino acids	$y = 0.0024x + 0.1903$	0.9692	5
carbohydrate	$y = 0.0044e^{0.0065x}$	0.6724	3
carnitines	$y = 0.1919\ln(x) - 0.3874$	0.8327	4
peptide	$y = 0.26967e^{0.0039x}$	0.8637	8
saturated fatty acid	$y = 0.0022x + 0.2515$	0.9665	13
unsaturated fatty acid	$y = 0.0023x + 0.2228$	0.9807	12